THE JOURNAL OF PHYSICAL CHEMISTRY B LETTERS

2006, *110,* 3856−3859
Published on Web 02/03/2006

Control of the ZnO Nanowires Nucleation Site Using Microfluidic Channels

Sang Hyun Lee,[†,*] Hyun Jung Lee,[§] Dongcheol Oh,[‡] Seog Woo Lee,[†] Hiroki Goto,[†] Ryan Buckmaster,[‡] Tomoyuki Yasukawa,[§] Tomokazu Matsue,[§] Soon-Ku Hong,[||] HyunChul Ko,[⊥] Meoung-Whan Cho,[†,‡] and Takafumi Yao[†,‡]

Center for Interdisciplinary Research, Tohoku University, Aramaki, Aoba-ku, Sendai 980-8578, Japan, Institute for Materials Research, Tohoku University, Katahira 2-1-1, Aoba-ku, Sendai 980-8577, Japan, Graduate School of Environmental Studies, Tohoku University, 07 Aramaki-Aoba, Aoba-Ku, Sendai 980-8579, Japan, Department of Materials Science and Engineering, Chungnam National University, Daejeon 305-764, Korea, and Department of Electrical and Computer Engineering, University of South Alabama, Mobile, Alabama 36688

Received: November 29, 2005; In Final Form: January 25, 2006

We report on the growth of uniquely shaped ZnO nanowires with high surface area and patterned over large areas by using a poly(dimethylsiloxane) (PDMS) microfluidic channel technique. The synthesis uses first a patterned seed template fabricated by zinc acetate solution flowing though a microfluidic channel and then growth of ZnO nanowire at the seed using thermal chemical vapor deposition on a silicon substrate. Variations the ZnO nanowire by seed pattern formed within the microfluidic channel were also observed for different substrates and concentrations of the zinc acetate solution. The photocurrent properties of the patterned ZnO nanowires with high surface area, due to their unique shape, were also investigated. These specialized shapes and patterning technique increase the possibility of realizing one-dimensional nanostructure devices such as sensors and optoelectric devices.

ZnO nanostructures are being investigated intensively because they possess powerful properties such as a direct wide band gap (3.37 eV), large excitation binding energy (60 meV),[1] and piezoelectric characteristics due to noncentral symmetry.[2] ZnO nanowires have been proven as useful materials in applications such as UV detectors,[3] lasers,[4,5] and light-emitting diodes.[6] To realize their full potential in, applications morphology control and integration methods are necessary. Various shapes of ZnO nanostructures have been reported previously such as nanowires,[3−5] nanobelts,[7] nanohelixes, nanosprings, and nanorings[8] grown by variety of methods such as a vapor−liquid−solid (VLS) processes using gold and metal catalyst,[4,5,9] wet chemical routes,[10] sol−gel electrophoretic deposition,[11] and metal organic vapor phase epitaxy (MOVPE).[12] Many methods for aligning nanowires have also been developed and can be categorized based on whether the alignment is done before or after the nanowire growth. Pre-growth alignment methods usually involve patterning the catalyst using dip-pen lithography,[13]microcontact printing,[14] templates.[15] Post-growth methods align the as-grown nanowires by Langmuir−Blodgett[16] or fluidic alignment techniques.[17,18] Among those, the microfluidic channel is a very powerful tool to align inorganic nanowires on substrate. The successful fabrication of two-dimensional (2D) parallel arrays and three-dimensional (3D) complex nanowire arrays on substrate was done using fluid flows within the channel as reported by Lieber and co-workers.[17,18] However, this method used horizontal flow of already-made nanowires within the channel. Therefore it is difficult to obtain vertical alignment or a large density of nanowires. Recently, Greene et al. has demonstrated a fabrication technique of ZnO nanowires on Si substrates using acetate-derived seeds for low cost solar cells.[19,20]

Here, we report a control technique of nucleation of ZnO nanostructures within a patterned area on substrate using the capillary force of zinc acetate solution in the microfluidic channels. Patterned zinc acetate solution transforms into nucleation seeds for ZnO nanostructures by heating. This technique shows the possibility of creating 1D nanostructured patterns for applications such as biosensors, piezoelectric devices, and optoelectronic devices.

The synthesis process involves three main steps. First, polydimethylsiloxane (PDMS) mold was prepared using a negative photoresist master (Micro Chem.). The pattern consists of four lines with 50 μm in width, 10 mm in length, and a 100 μm separation between the lines. The pattern was transferred to the substrate by previously established techniques by curing the prepolymer on template with a master[21] (step 1 in Figure 1). Second, the patterned PDMS mold was carefully placed on a clean substrate to form rectangular microfluidic channels. The zinc acetate dehydrate was diluted with ethanol to 0.005 M. A 2 μL portion of diluted zinc acetate solution was dropped at one side of each channel, and the solution flowed rapidly to

* Corresponding author. Tel: +81-22-795-4404. Fax: +81-22-795-7810. E-mail:shlee@cir.tohoku.ac.jp.
† Center for Interdisciplinary Research, Tohoku University.
‡ Institute for Materials Research, Tohoku University.
§ Japan Graduate School of Environmental Studies, Tohoku University.
|| Department of Materials Science and Engineering, Chungnam National University.
⊥ Department of Electrical and Computer Engineering, University of South Alabama.

10.1021/jp056915n CCC: $33.50

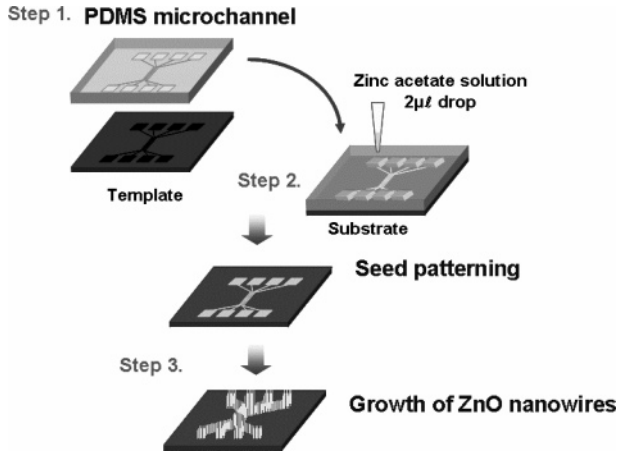

Figure 1. Schematic of zinc acetate solution patterning using PDMS microfluidic channels. First, microfluidic channels are formed from the molding template and surface of substrate (Step 1). Then ZnO seeds are patterned by injection of zinc acetate solution into the channels and heating (Step 2). Finally, the ZnO nanowires were grown from patterned seeds using thermal chemical vapor deposition (Step 3).

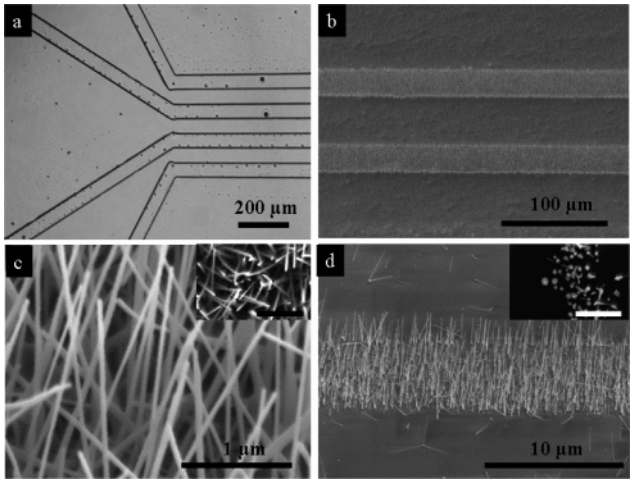

Figure 2. (a) Optical microscope image of PDMS microchannels. (b, c) SEM images of a 50 μm line patterned, (d) 45 tilted view and top view SEM images (inset) of a 5 μm line of patterned ZnO nanowires on a SiO_2/Si substrate. Scale bar in inset image; 1 μm.

the other side by capillary force. This solution injection step was repeated for all channels. The patterned zinc acetate solution on the substrate was dried in air at 70 °C to eliminate the solvent. After detachment of the PDMS mold from the substrate, the patterned substrate was heated at 250 °C for 10 min. Through this heating process in air, the zinc acetate decomposed into ZnO nanoparticles, to function as nucleation seeds for ZnO nanostructure growth. Finally, ZnO nanowires were synthesized on the substrate by thermal chemical vapor deposition using a mixture of zinc oxide and carbon powder at 910 °C for 30 min.

Figure 2 shows the optical image of the PDMS molder (Figure 2a) and the resulting growth of two channels (Figure 2b,c). The top-view SEM image (Figure 2b) shows that the ZnO nanowire nucleation area is the same as the PDMS mold. The top and tilt view SEM images (Figure 2c and inset images) show the magnified image of the line pattern, which consists of well-faceted ZnO nanowires of 20∼80 nm in diameter and 7∼10 μm in length. There are various growth orientations and some connections into adjacent nanowires at the tip or branch. This result shows the different morphology with vertical ZnO nanorods using zinc acetate seed by Yang and co-workers.[19] We also fabricated 5 μm line patterns of the vertically aligned ZnO nanoneedles of 10∼100 nm in diameter and 2∼3 μm in length on Si substrate shown in Figure 2d. ZnO nanoneedles show lower density than that of nanowires and are free-standing grown on substrate. The shapes of ZnO nanostructures are strongly dependent on morphology of zinc acetate seeds. The formation of zinc acetate seeds is very sensitive to process conditions including injection and heating time. On thrice repeating the zinc acetate solution injections and heating steps, ZnO nanowires with large density and random growth directions on the patterned lines were observed. Different from this case, however, though only one injection and heating step, vertically aligned ZnO nanoneedles with low density were formed.

To know the output of pattern shapes and solution concentrations, we conducted the synthesis according to four different concentrations of zinc acetate solution which were 5×10^{-6}, 5×10^{-5}, 5×10^{-4}, and 5×10^{-3} M, respectively. Solution was injected into four channels and then quickly dried on substrate at 70 °C in air atmosphere. Figure 3 shows the top-view SEM images of each pattern with ZnO nanowires on a Si(100) substrate. The top and bottom images of Figure 3a−d show the entrance and the middle part of each channel, respectively. At a high concentration (5×10^{-3} M), the channel is completely filled with ZnO nanowires over the whole patterned line (Figure 3d). In the case of lower concentrations (Figures 3a−c), the pattern was separated into two parallel lines within the microchannels. This separation phenomenon within the channel mostly occurred at the middle part rather than the input point of the channel, as shown in upper and lower images in Figure 3b and

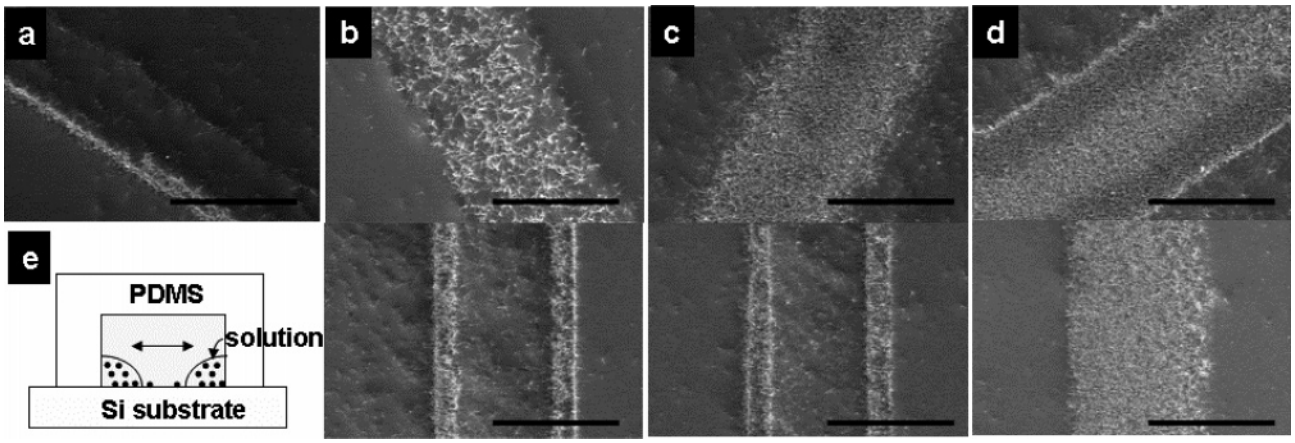

Figure 3. SEM images of ZnO nanowires pattern with various concentrations of zinc acetate solutions. The concentrations are (a) 5×10^{-6}, (b) 5×10^{-5}, (c) 5×10^{-4}, and (d) 5×10^{-3}M, respectively. Scale bar is 50 μm.

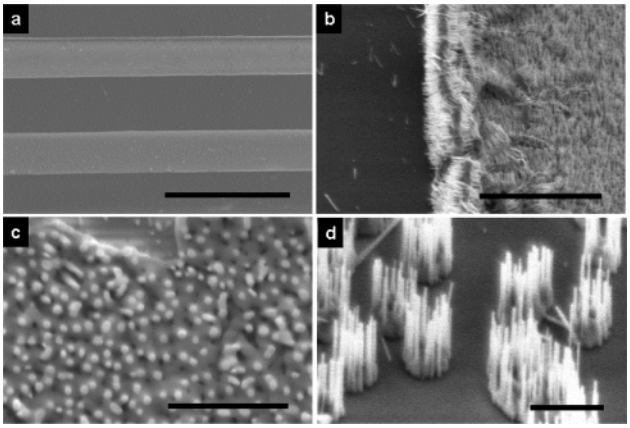

Figure 4. SEM images of ZnO nanowires line patterns and edge part being on Al_2O_3 substrate (a), (b), (c) top and (d) 45° tilting view. Scale bar: 200, 5, 1, 1 μm, respectively.

3c. It is likely that the driving force is different at each part of the channel, inlet, outlet, and midpoint, respectively. Both the injection pressure and capillary force are present at the inlet, however only capillary force functions at the outlet. The ZnO nanowires were uniformly distributed with line width of 5 μm and gap of 50 μm, which reflect the features of the mircofluidic channels with 50 μm width. These lines are formed by movement of the colloid, which is expected to recede into two corners of the channel, and that the solution near the corners becomes concentrated during solvent evaporation via capillary force (Figure 3e). As a result, the line patterns of ZnO seed in zinc acetate solution are indeed aligned along the edge of the channels during dewetting. Other groups have also used the dewetting process within microchannels to align inorganic nanowires and carbon nanotubes.[22,23]

When well-polished Al_2O_3 (1000) were used as a substrate via the same procedures, line patterns of vertically aligned ZnO nanowires 10∼20 nm in diameter and ∼1 μm in length were obtained (Figure 4a), although with a high density of edge and partially nonuniform coverage (Figure 4b−d). Zinc acetate solution could not be wet uniformly at the surface of Al_2O_3 substrate due to hydrophobic properties. A droplet with a high contact angle with the substrate is formed at the edges of the channel. (Figure 3e).

Transmission electron microscopy (TEM) studies were carried out to examine in detail the surface morphology and crystallography of the ZnO nanowires grown on SiO_2/Si substrate. At low magnification, TEM images (Figure 5a) of the ZnO nanowires correspond with SEM results; in addition, we can confirm that the surface of nanowires is very smooth also. The high magnification images reveal rugged surface morphology a large surface area (Figures 5b and 5c). Figure 5c shows high-resolution transmission electron microscopic (HRTEM) image and corresponding electron diffraction pattern taken at the tip of the ZnO nanowires. Both nanoblock and body of the nanowires have a lattice spacing of $c = 0.52$ nm, which is compatible with the standard values of ZnO bulk crystal, and grew along the [0001] direction. The TEM results indicate that ZnO nanowires are a single crystal. The large surface area is due to 3D structures such as the nanoblocks on the nanowires as represented in Figure 5d. A possible growth mechanism is the decomposition of ZnO into Zn vapors and oxygen at high temperatures or self-catalyzed growth.

A UV response detector applying the patterns of the unique nanoblock shaped ZnO nanowire with high surface area was fabricated with the configuration shown in Figure 6a inset. Two electrodes were formed by evaporating Ti (10 nm) and Au (30 nm) at each end of a line of patterned ZnO nanowires (Figure 6a inset). Current−voltage ($I-V$) characteristics, photocurrent, and photoluminescence (PL) were evaluated at room temperature. Figure 6a shows $I-V$ characteristics of the photocurrent excited at different UV light intensities from a Halogen lamp with a maximum power (I_{max}) of 100 W and also the dark current as a reference. The nonlinear $I-V$ curve might originate from contact barriers between the metal electrodes and ZnO nanowires or between each ZnO nanowire. It has been suggested that the $I-V$ curve of ZnO nanowires with Au electrodes change from Ohmic to Schottky contacts under different light sources (325 and 485 nm), which are above and below band gap, respectively.[24] This was explained by the electron tunneling into the narrow width of the Schottky barrier between the electrode and surface of ZnO nanowires. However, our results showed that the nonlinear $I-V$ curves are observed regardless of the UV illumination. It might be due to the existence of small gaps between each nanowire as well as Schottky barriers between the electrode and ZnO nanowires. It is difficult for electrons to pass the line of ZnO nanowires within a low electric field, except to overcome the energy barrier by electron tunneling in a high electric field. Figure 6b shows the photoresponse spectrum under modulated illumination of a 450W Xe lamp with a monochromator having a wavelength range from 300 to 600 nm. A bias voltage of 2.5 V was applied between the two electrodes. For comparison, the PL spectrum of the patterned ZnO nanowires is also shown in Figure 6b. The photocurrent was measured by a HP 34401 multimeter. The edge of photocurrent observed at 410 nm (3.26 eV) corresponded to the minimum value of PL data. It indicates that the excitons are exited by UV light and produce the photocurrent. The photocurrent curve shows a maximum value at 335 nm. This value is close to the electronic density of states near the conduction band edge. A broad

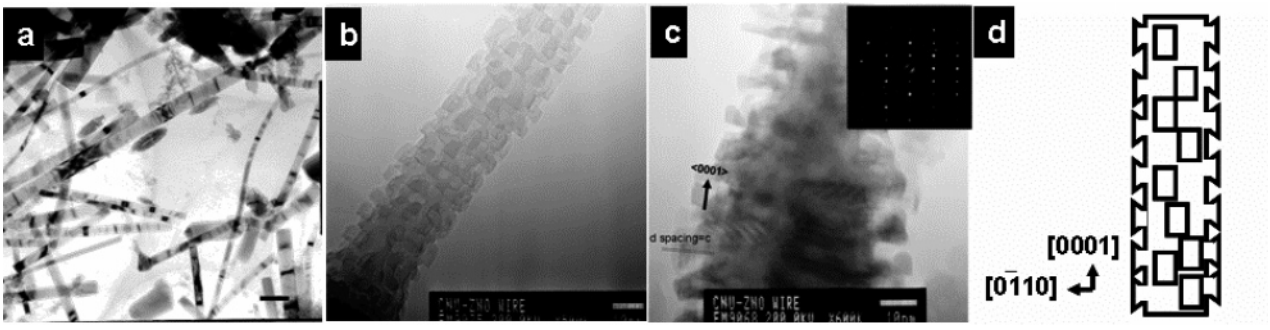

Figure 5. TEM images of ZnO nanowires (a) low-magnification image, (b) high-magnification image taken on the body of ZnO nanowire, (c) HRTEM image at tip of nanowire and corresponding diffraction pattern, (d) schematic drawing of side view of part of a nanowire. Scale bar: 100, 10, and 10 nm, respectively.

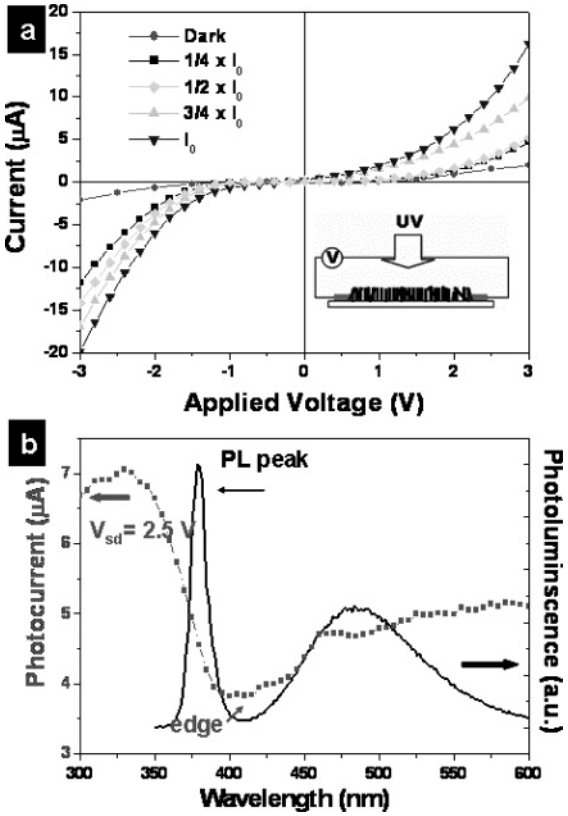

Figure 6. (a) Current−voltage characteristics with variation of UV density and schematic of photocurrent measurement. (b) Photocurrent at 2.5 V drain-source bias (V_{ds}) and photoluminescence of patterned ZnO nanowires.

photocurrent and PL peak at 480 nm is also observed, which is caused by native defect levels within the band gap, such as single and double ionized oxygen vacancies.[25,26]

In summary, we suggest unique and a more efficient method for synthesizing ZnO nanowires using PDMS microfluidic channels. The pattern morphology is controlled by the injection and heating process according to the solution's concentration and the interactions between the substrate and solution. It was verified from TEM studies that the surface morphologies of ZnO nanowires grown on the Si substrate exist in the shape of 3D structures such as nanoblocks on nanowires. Furthermore, we fabricated a UV detector by applying the patterned ZnO nanowires with the unique surface structure and demonstrated its application potentials as a sensitive UV detector. Our selective growth of ZnO nanowires with large surface area and the simple control technigue of the pattern morphology using microfluidic channels have great potential for nanodevices and systems along with possible applications for other nanostructures.

Note Added after ASAP Publication. This article was published ASAP on February 3, 2006. The caption to Figure 4 has been modified. The correct version was posted on February 6, 2006. The captions to Figures 4 and 5 have since been further modified. This version was posted on February 10, 2006.

References and Notes

(1) Chen, Y.; Bagnall, D. M.; Koh, H.; Park, K.; Hiraga, K.; Zhu, Z.; Yao, T. *J. Appl. Phys.* **1998**, *84*, 3912.
(2) Yamamoto, T.; Shiosaki, T.; Kawabata, A. *J. Appl. Phys.* **1980**, *51*, 3113−3120.
(3) Kind, H.; Yan, H.; Messer, B.; Law, M.; Yang, P. D. *Adv. Mater.* **2002**, *14*, 158−160.
(4) Huang, M.; Mao, S.; Feick, H.; Yan, H. Q.; Wu, Y. Y.; Kind, H.; Weber, E.; Russo, R.; Yang, P. D. *Science* **2001**, *292*, 1897.
(5) Johnson, J. C.; Yan, H.; D. Schaller, R, D.; Haber, L. H.; Saykally, R. J.; Yang, P. D. *J. Phys. Chem. B* **2001**, *105*, 11387−11390.
(6) Liu, C. H.; Zapien, J. A.; Yao, Y.; Meng, A. M.; Lee, C. S.; Fan, S. S.; Lifshitz, Y.; Lee, S. T. *Adv. Mater.* **2003**, *15*, 839−841.
(7) Pan, Z, W.; Dai, Z. R.; Wang, Z. L. *Science* **2001**, *291*, 1947−1949.
(8) Kong, X. Y.; Wang, Z. L. *Nano Lett.* **2003**, *3*, 1625−1631.
(9) Gao, P. A.; Ding, Y.; Wang, Z. L. *Nano Lett.* **2003**, *3*, 1315−1320.
(10) Vayssieres, L. *Adv. Mater*. **2003**, *15*, 464−466.
(11) Wang, Y. C.; Leu, I. C.; Hon, M. H. *J. Cryst. Growth* **2002**, *237−239*, 564−568.
(12) Park, W. I.; Yi, G. C.; Kim, M.; Pennycook, S. J. *Adv. Mater.* **2002**, *14*, 1841−1843.
(13) Piner, R. D.; Zuh, J.; Xu, F.; Hong, S.; Mirkin, C. A. *Science* **1999**, *283*, 661−663.
(14) Kind, H.; Bonard, J.-H.; Emmenegger, C.; Nilsson, L.-O.; Hernadi, K.; Maillard-Schaller, M.; Schlapbach, L.; Forro, L.; Kern, K. *Adv. Mater* **1999**, *15*, 1285−1289.
(15) Wang, X.; Summers, C. J.; Wang, Z. L. *Nano Lett.* **2004**, *4*, 423−426.
(16) Whang, D.; Jin, S.; Wu, Y.; Lieber, C. M. *Nano Lett.* **2003**, *3*, 1255−1259.
(17) Huang, Y.; Duan, X.; Wei, Q, Lieber, C. M. *Science* **2001**, *291*, 630−633.
(18) Cui, Y.; Lieber, C. M. *Science* **2001**, *291*, 851−853.
(19) Green, L. E.; Law, M.; Tan, D. H.; Montano, M.; Goldberger, G.; Somorgai, G.; Yang, P. *Nano Lett.* **2005**, *5*, 1231−1236.
(20) Law, M.; Green, L. E.; Johnson, J. C.; Saykally, R.; Yang, P. D. *Nature Mater.* **2005**, *4*, 455−459.
(21) Nagamine, K.; Onodera, S.; Torisawa, Y.-S.; Yasukawa, T.; Shiku, H.; Matsue, T. *Anal. Chem.* **2005**, *77*, 4278−4281.
(22) Messer, B.; Song, J. H.; Yang, P. D. *J. Am. Chem. Soc.* **2000**, *122*, 10232−10233.
(23) Chen, J.; Weimer, W. A. *J. Am. Chem. Soc.* **2002**, *124*, 758−759.
(24) Keem, K.; Ki, H.; Kim, G.-T.; Lee, J. S.; Min, B.; Cho, K.; Sung, M.-Y.; Kim, S. *Appl. Phys. Lett.* **2004**, *84*, 4376−4378.
(25) Vanheusden, K.; Warren, W. L.; Seager, C. H.; Tallant, D. R.; Voigt, J. A.; Gnade, B. E. *J. Appl. Phys.* **1996**, *79*, 7983−7990.
(26) Lin, B.; Fu, Z.; Jia, Y. *Appl. Phys. Lett.* **2001**, *79*, 943−945.